Test Structure for Evaluation of Pad Size for Wafer Probing

Brad Smith[1], Donald Hall[1], and Garrett Tranquillo[2]
[1] *NXP Semiconductors*, Austin, TX, USA
[2] *Celadon Systems, Inc*., Burnsville, MN, USA
brad.smith@nxp.com

***Abstract*—A new, cage-like structure is presented and is shown to be able to electrically identify a probe needle that has fallen slightly off its probe pad, even when the standard probe resistance structure (pads shorted together) reports "good" probe resistance. Using both structures together enables a more accurate evaluation of a probe system's capabilities. Both test structures were used to compare three types of probe cards, reporting the smallest probe pad size that provides 100% probe yield.**

Keywords—wafer probe, test structure, probe pad size

I. Introduction

In wafer probe, a common method for assessing proper contact of the probe needles to the probe pads is to measure needle-to-needle resistance using a structure in which the pads are intentionally shorted together (Fig. 1). If the needles are sitting on the pads, a low resistance between them should be measured. Any resistance above a chosen value is considered an "open" and is called a failure. This method is effective for catching dirty or damaged probe needles and can be used to trigger a probe needle cleaning or repair cycle. In this work, this structure will be referred to as the "shorts" structure since the probe needles will be shorted when functioning properly.

There have been numerous published studies of wafer probing and probe resistance, but most tend to focus on lower probe resistance [1]-[4], the physics of the needle-on-pad contact [5]-[8], or the impact that wafer probing has on yield [9]-[12] and/or assembly [13]-[16]. Based on anecdotal evidence, it is believed that the use of the aforementioned structure with its pads shorted together is ubiquitous.

If a probe needle has partially fallen off its pad but is still making some contact, it could be measured as "good". For inline probe (i.e., probing done before wafer processing is complete), a probe needle that is slightly off the probe pad could be shorted to a neighboring metal line while still measuring as "good" probe resistance. For an end-of-line probe on passivated pads, this may or may not be acceptable, as any neighboring lines will be passivated and should be protected from the probe needles. That said, a probe needle hitting passivation could cause cracks, which could become a reliability issue [17]. Therefore, another type of structure is needed to catch this failure mode.

II. New Structure

A new, cage-like structure has been developed to catch when a probe needle has shorted to a metal feature near the probe pad. Two implementations are shown in Fig. 2. The first requires one pad as a "witness" that is used to detect a probe needle that is slightly off any of the other probe pads (Fig. 2a). This would measure as a short to the "witness" pad. The wire from each probe pad to the "witness" pad could potentially be millimeters long and a high resistance there could reduce the ability of the structure to detect a short. In addition, a misaligned needle for that "witness" pad cannot be included in the measurement of probe needle misalignment.

Ideally, the series resistance between the probe pads would be minimized and all probe pads would be testable for shorts to neighboring wires (i.e., one pad not sacrificed to act as "witness" for all the others). Fig. 2b shows the cage structure used for the majority of this work, which satisfies both of these requirements. Each pad can be measured for probe needle misalignment and also acts as a "witness" for the probe needle misalignment on neighboring pads. The resistance from each probe pad to its adjacent pads is measured, with "good" defined as measuring a high value, indicating no shorting. This structures works for probe pads that are larger than the width used for the "witness" lines. For very small pads, the structure in Fig. 2a would be preferable. In either format, this type of structure shall be referred to as the "opens" structure since the probe needles will be electrically open when functioning properly.

The structures described here could be used for any sort of probe card qualification, including routine production monitoring of probe hardware. The ability to measure opens and shorts for each probe needle enables identification of issues with individual probe needles. In addition, these

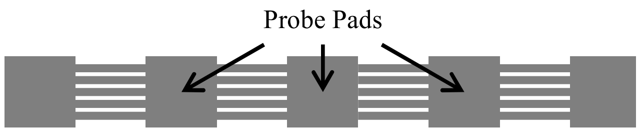

Fig. 1 Industry-standard probe resistance structure for "shorts" measurements.

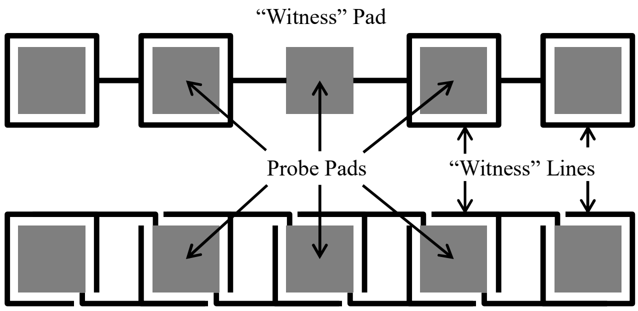

Fig. 2 The new cage-style "opens" structures used in this work. In (a), measuring a short between any pad and the "witness" pad indicates that the probe needle has fallen slightly off its probe pad. In (b), every pad acts as the "witness" for its neighboring pad(s).

979-8-3503-4653-4/23/$31.00 ©2023 IEEE

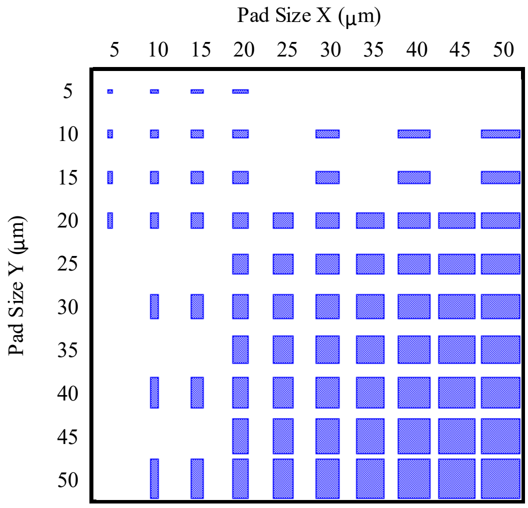

Fig. 3 The 76 probe pad sizes measured for this experiment.

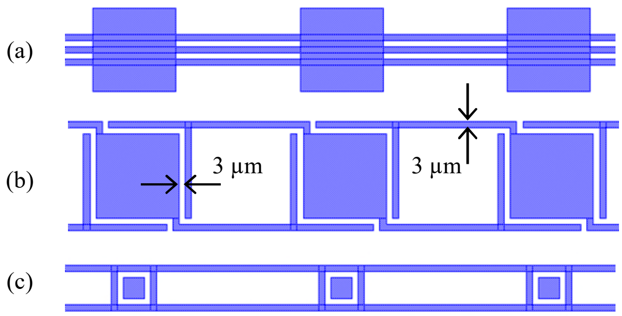

Fig. 4 Example layouts of the structures used in this work: (a) "shorts", (b) cage "opens" for pad sizes of 20 μm or more, and (c) cage "opens" for pad sizes of 20 μm and smaller.

structures can be used for comparisons of probe cards and/or probers to assess their capabilities.

III. Experimental

"Shorts" and "opens" pad structures from Fig.s 1 and 2 were built in unpassivated aluminum using a 90 nm technology on 200 mm wafers. As shown in Fig. 3, probe pad size was varied in a full matrix of widths and heights of 20, 25, 30, 35, 40, 45, and 50 μm, plus a partial matrix of pad widths and heights down to 5 μm. The witness lines were 3 μm wide and were 3 μm from the probe pads. All structures had 22 pads in a single line with a pitch of 100 μm. These pads were left unpassivated to maximize sensitivity to a probe needle shorting to a neighboring witness line.

Fig. 4 shows example layouts of these structures. For the pad sizes of 20 μm and below, alternate layouts were used (Fig. 4c) because the pad dimensions were comparable to the minimum with rule for aluminum.

Both the "shorts" and "opens" types of structures were measured on every pad, using the probe procedure from [18], including the 10 μm target scrub length. For analysis, the measured resistances for each structure and probe pad were first converted into a 1 for "pass" or 0 for "fail". The criteria used for "pass" was probe resistance $\geqslant$ 1 MΩ for the "opens" structures and $\leqslant$ 10 Ω for the "shorts" structures. Taking the average of these values provides a probe yield, either per pin or per probe card (22 pins).

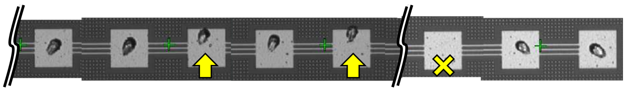

Fig. 5 Photo of the probe scrub marks made by a damaged probe card with bent needles. One probe pin didn't touch its probe pad at all and two others were misaligned in the Y direction.

A. Structure Verification

The first experiment was intended to verify that the new cage structure did what is was designed to do – to detect a probe needle falling off its probe pad. Three die were probed at 25 °C using a damaged probe card with bent needles (Fig. 5). One needle on this probe card was so bent that it didn't make contact with its probe pad at all. Two other needles were bent roughly 12 μm and 20 μm in the direction perpendicular to the row of probe pads (i.e., vertical in Fig. 5). The intended output was to measure how well the "shorts" and "opens" test structures responded to various amounts of probe needle misalignment so different probe pad sizes were used as a substitute for multiple probes with intentional misalignment.

B. Probe Card Comparison

The second experiment compared three styles of cantilever probe card: interlaced (the industry standard, which has probe needles coming from two sides), a one-sided card, and an experimental low-scrub, one-sided probe card. Photos of the interlaced and one-sided styles and the "scrub" marks they make on probe pads are shown in Fig. 6. Five die were probed at 25, 125, and 175 ºC. Note that while 76 probe pad sizes were measured each time, only the square sizes (where X=Y) are shown in the plots for brevity. The desired output was determination of the smallest square probe pad size that each probe card was capable of probing reliably at multiple temperatures.

IV. Results

A. Structure Verification

Using the damaged probe card, the probe needle that didn't make contact with its probe pad failed the "shorts" structure and passed the "opens" structure, as expected. This is where the standard "shorts" structure works well, detecting bad probe needles. The "opens" structure detected an open, so passed.

The probe yields for the two bent probe needles are shown in Fig. 7 as a function of probe needle position with respect to the probe pad. Photos of the probe scrub marks are included

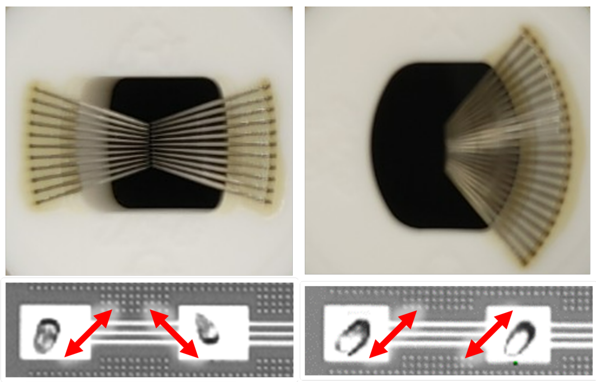

(a) Interlaced (b) One-sided

Fig. 6 Photos of the types of probe cards compared in this work and example scrub marks made by each.

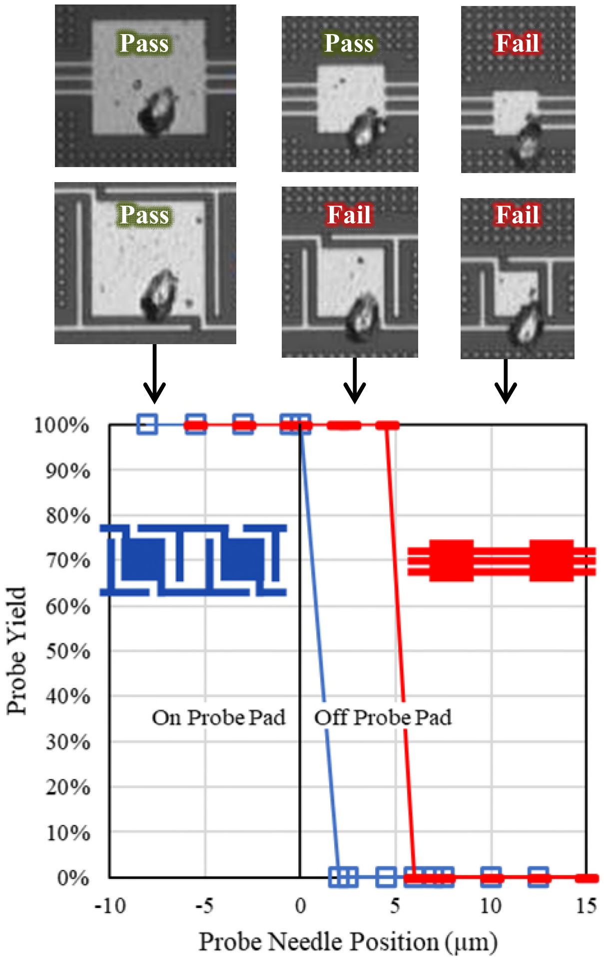

Fig. 7 Probe yield as a function of probe needle distance from the edge of the probe pad. Error bars for the probe needle misalignment measurements are not shown for clarity, but are estimated to be +/- several microns.

for clarity. The position of the center of the probe needle was estimated from the scrub mark photos and then the distance to the edge of the pad was calculated. These are fairly crude measurements, with a resolution estimated to be +/- several microns, but they should still enable comparison of the two test structures. When the probe needle landed completely on the probe pad, both the "shorts" and "opens" structures passed. When the probe needle partially fell off its probe pad, the standard "shorts" structure still passed while the new "opens" structure failed. When the probe needle was completely off its probe pad, the "opens" structure continued to fail but probe needle fell far enough off its pad that the "shorts" structure also failed.

To compare how the two test structures respond to the full matrix of probe pad sizes, Fig. 8 shows probe yields measured at 25ºC for the industry-standard interlaced probe card. Both structures yielded 100% for large pads (lower right corner of the tables), but the "opens" structure yield had a smaller region with 100% yield. Viewing the matrix in this form also provides insight into how rapidly the probe yield drops off as probe pad size is reduced.

B. *Probe Card Comparison*

Fig. 9 shows probe yield for the interlaced probe card as a function of temperature for a 25x25 µm probe pad. Unsurprisingly [19], higher temperatures produced lower

Pad Size Y (µm) \ Pad Size X (µm)	5	10	15	20	25	30	35	40	45	50
5	89%	90%	88%	86%						
10	85%	88%	89%	92%		94%		94%		94%
15	93%	89%	92%	91%		94%		94%		94%
20	87%	91%	90%	92%	91%	94%	95%	94%	92%	95%
25				94%	93%	95%	95%	95%	95%	95%
30		90%	90%	94%	95%	92%	100%	100%	100%	95%
35				100%	100%	100%	100%	100%	100%	100%
40		91%	87%	100%	100%	100%	100%	100%	100%	100%
45				100%	100%	100%	100%	100%	100%	100%
50		86%	91%	95%	94%	95%	100%	100%	100%	100%

(a) Shorts at 25 °C

Pad Size Y (µm) \ Pad Size X (µm)	5	10	15	20	25	30	35	40	45	50
5	2%	12%	16%	18%						
10	27%	63%	59%	52%		64%		59%		57%
15	28%	77%	63%	58%		61%		55%		59%
20	33%	66%	58%	72%	64%	65%	65%	78%	80%	85%
25				82%	84%	82%	82%	82%	82%	82%
30		67%	82%	82%	82%	82%	82%	82%	82%	82%
35				82%	82%	82%	100%	100%	100%	100%
40		69%	76%	73%	73%	73%	100%	100%	100%	100%
45				91%	91%	91%	100%	100%	100%	100%
50		73%	72%	82%	82%	82%	100%	100%	100%	100%

(b) Opens at 25 °C

Legend: 0+% 70+% 90+% 100%

Fig. 8 Probe yield for the full matrix of probe pad sizes, measured at 25 °C using the industry-standard interlaced probe card. (a) is the standard "shorts" structure, and (b) is the new "opens" structure.

probe yields. Subsequent plots shall focus on the 175 ºC measurements, since that is worst case.

Fig. 10 shows probe yield for the standard "shorts" structure as a function of square probe pad size for the three probe cards described earlier. Minimum probe pad size was 35x35 µm for the interlaced probe card and 20x20 µm for the one-sided probe card. The experimental, low-scrub probe card did not fail for any probe pad size down to 5x5 µm.

The corresponding plot using the new "opens" structure is shown in Fig. 11. The minimum probe pad sizes were 35x35 µm for the interlaced probe card, 25x25 µm for the one-sided probe card, and 15x15 µm for the low-scrub probe card. For the interlaced and one-sided probe cards, these were

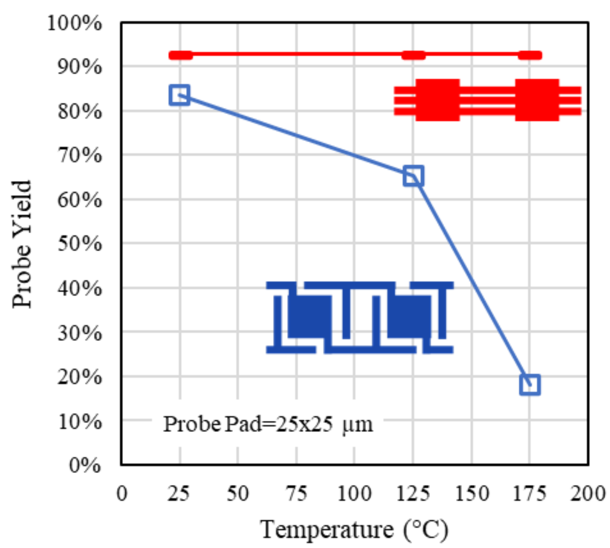

Fig. 9 Probe yield of the industry-standard interlaced probe card as a function of temperature for 25x25 µm probe pads. As expected, probe yield dropped with increasing temperature.

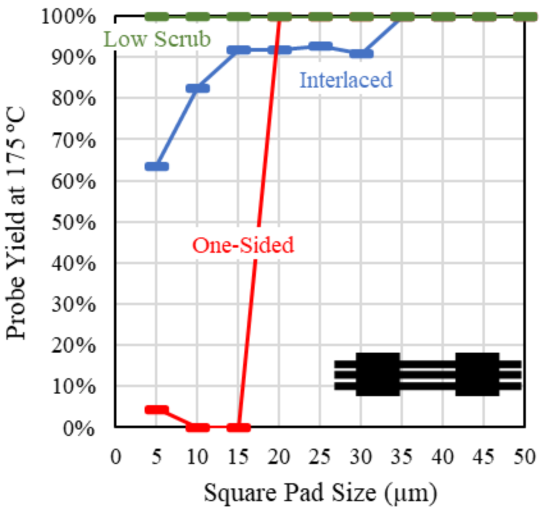

Fig. 10 Probe yield as a function of square pad size for three types of probe card using the standard "shorts" structure. Minimum probe pad size is the smallest pad that has 100% probe yield.

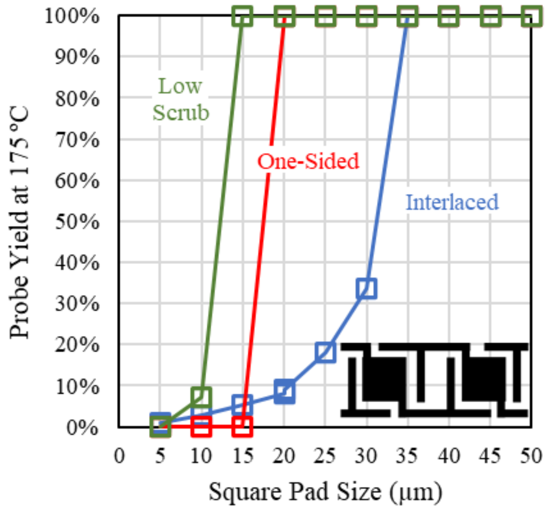

Fig. 11 Probe yield as a function of square pad size for three types of probe card using the new "opens" structure. Minimum probe pad size is the smallest pad that has 100% probe yield.

the same values as found with the standard "shorts" structure. For the low-scrub probe card, the "shorts" structure did not find any failures, even down to 5x5 µm, but the "opens" structure failed below 15x15 µm.

V. Discussion

A. Test Structure Comparison

For the traditional "shorts" structure to fail, the probe needle apparently needs to fall completely off the probe pad. These probe needles were around 7 µm in diameter, so having the probe yield drop to zero for distances of more than 5 µm from the pad edge is within the measurement error of the distance. Fig. 12 re-plots the measurements from Fig. 7 to show the measured probe resistance instead of probe yield. The probe resistance was an acceptable value (≤10 Ω) even when the probe needles were a few microns off the edge of the probe pads. Any farther off the pad and the resistances jumped immediately to GΩ (i.e., open). Thus, the standard "shorts" structure worked well for detecting a probe needle that's completely off its probe pad, but falsely read as "good" resistance when the probe needle was partially off the pad.

The plot in Fig. 7 shows the expected electrical behavior for the new "opens" structure. The photos in Fig. 7 confirm that the "witness" lines surrounding each pad electrically detected when a probe needle was slightly off its probe pad. Thus, this cage structure is more sensitive to probe needles falling slightly off their probe pads than the standard "shorts" structure. That said, it falsely reported as "good" when the probe needle made no contact at all. And, of course, this structure cannot report probe resistance, since "good" here means no electrical connection between neighboring probe pads.

Each type of probe structure reports different failure mechanisms so ideally, both would be used to evaluate a probe system. The "shorts" structure can detect a probe needle not making good contact to its probe pad but can give false "good" readings if the needle does not land completely within the probe pad. The "opens" structure can detect that case, but gives a false "good" reading if the probe needle makes no contact at all. It is common within the industry to use the "shorts" structure by itself, but adding the new cage-style "opens" structure can address its known weakness.

B. Probe Card Comparison

The standard interlaced probe card was shown to be capable of probing square pads down to 35x35 µm at 175 °C, while the one-sided probe card was capable of 20x20 µm. The interlaced probe card was designed with its probe needle placements staggered by 14 µm to compensate for their complementary scrub directions, as is common practice. The one-sided probe card, by contrast, was designed with its probe needles in a straight line. The comparison is shown in Fig. 13. This means the interlaced probe card should require a 15 µm

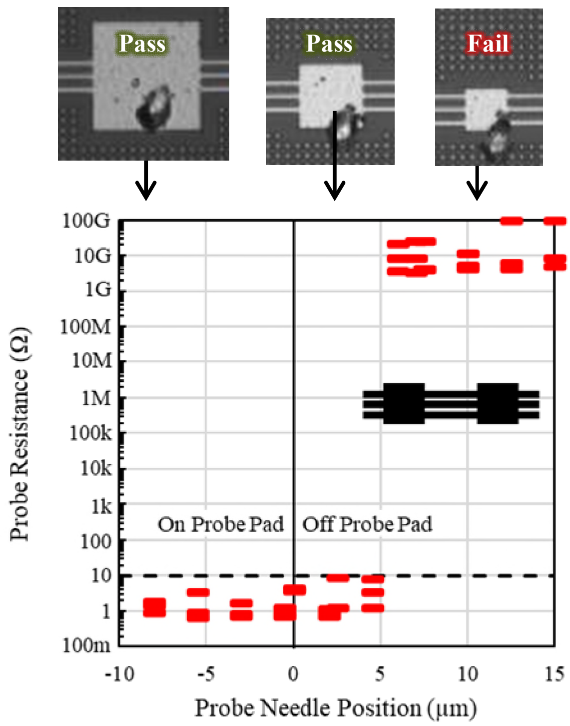

Fig. 12 Probe resistance as a function of probe needle distance from the edge of the probe pad. Resistance was <10 Ω when the probe needle was on the probe pad and even when it was a few microns off, but jumped to GΩ for more than a few microns off the probe pad.

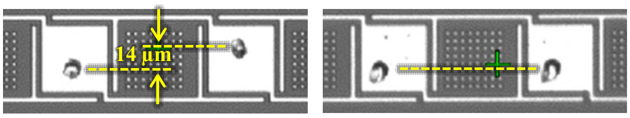

(a) Interlaced probe card (b) One-sided probe card

Fig. 13 Probe scrub marks for the interlaced and one-side probe cards. The interlaced probe card was designed with staggered probe needle placements (a common practice), whereas the one-sided card's probe needles were designed to be in a straight line. This is why the interlaced probe card required larger probe pads than the one-sided probe card.

larger probe pad than the one-sided card, and the measurements agree extremely well. The experimental, low-scrub probe card was shown to be able to probe 15x15 µm probe pads, a modest improvement over the one-sided probe card. The data from this experiment did, however, provide insights into design improvement options for the next revision of that probe card (the possible subject of a future publication).

VI. Conclusion

A new cage-like "opens" structure has been defined and verified that it electrically detects when a probe needle partially contacts its probe pad but also shorts to a neighboring wire. The standard "shorts" structure (pads shorted together) was shown to report acceptable probe resistance even when a probe needle was slightly off its probe pad. The new cage structure, however, cannot measure probe resistance or detect when a probe needle makes no contact to its probe pad. Thus, using both structures produces the most accurate assessment of a wafer probe system. Both structures were used to compare three types of probe card, producing plots of probe yield as a function of probe pad size. The measurements confirmed that an the interlaced probe card, which had probe pins with staggered alignment, required 15 µm larger probe pads than the one-sided probe card, consistent with the probe cards' designs. A third, experimental one-sided probe card was also measured and shown to enable slightly smaller probe pads than the one-sided probe card.

VII. Acknowledgement

The authors wish to thank Dalton Roehl (Celadon), who was critical to design the low-scrub probe card.

References

[1] J. J. Broz and R. M. Rincon, "Probe contact resistance variations during elevated temperature wafer test", *International Test Conference 1999. Proceedings (IEEE Cat. No.99CH37034)*, 1999, pp. 396-405, doi: 10.1109/TEST.1999.805761.

[2] C. B. Sia, "True Kelvin CMOS Test Structure to achieve accurate and repeatable DC wafer-level measurements for device modelling applications", *2017 Int'l Conference of Microelectronic Test Structures (ICMTS)*, 2017, pp. 1-4, doi: 10.1109/ICMTS.2017.7954268.

[3] R. Trahan, R. Kiang and A. Frerichs, "Optimizing the die probe process using Taguchi techniques", *[1992 Proceedings] IEEE/SEMI International Semiconductor Manufacturing Science Symposium*, 1992, pp. 7-12, doi: 10.1109/ISMSS.1992.197627.

[4] H. Li and D. Zheng, "Study on Retest Reduction by Minimizing Probe Card Contact Resistance at Wafer Test", *2021 China Semiconductor Technology International Conference (CSTIC)*, 2021, pp. 1-4, doi: 10.1109/CSTIC52283.2021.9461487.

[5] W. Tang, M. R. Gomez, Y. Y. Lau, R. M. Gilgenbach, and J. Zier, "Theory and experimental measurements of contact resistance", *2009 IEEE International Conference on Plasma Science - Abstracts, 2009*, pp. 1-1, doi: 10.1109/PLASMA.2009.5227509.

[6] O. Nagler, T. Krebs and M. Heuken, "An Improved Model of Electrical Contact Resistance of Pad-Probe Interaction during Wafer Test", *2019 IEEE Holm Conference on Electrical Contacts*, 2019, pp. 68-75, doi: 10.1109/HOLM.2019.8923892.

[7] D.-S. Liu, M.-K. Shih, and F.-M. Zheng, "An Investigation of Wafer Probe Needles Mechanical Properties and Contact Resistance Changing Under Multiprobing Process", in *IEEE Transactions on Components and Packaging Technologies*, vol. 31, no. 1, pp. 196-203, March 2008, doi: 10.1109/TCAPT.2008.916856.

[8] A. M. Yassine, T. M. Clien and B. A. Beitman, "Characterization of probe contact noise for probes used in wafer-level testing", in *IEEE Electron Device Letters*, vol. 12, no. 5, pp. 200-202, May 1991, doi: 10.1109/55.79555.

[9] S. Lee, B. Kim, J. Park, S. Yoo and J. Jeon, "The method for measurement of the real overdrive: YE: Yield enhancement/learning", *2017 28th Annual SEMI Advanced Semi. Manufacturing Conference (ASMC)*, 2017, pp. 230-233, doi: 10.1109/ASMC.2017.7969236.

[10] N. Nadeau and S. Perreault, "An analysis of tungsten probes' effect on yield in a production wafer probe environment", *Proceedings. 'Meeting the Tests of Time'., International Test Conference*, 1989, pp. 208-215, doi: 10.1109/TEST.1989.82296.

[11] E. Ramanathan *et al*., "Study of Probe Contact Resistance Impact on Inline Testing with Different Bond Pad Design in BEOL", *2019 30th Annual SEMI Advanced Semiconductor Manufacturing Conference (ASMC)*, 2019, pp. 1-4, doi: 10.1109/ASMC.2019.8791826.

[12] G. T. Placido, C. Olalia, and R. Alolod, "Six sigma: Systematic approach in probe damage reduction", *36th International Electronics Manufacturing Technology Conference*, 2014, pp. 1-6, doi: 10.1109/IEMT.2014.7123114.

[13] G. Hotchkiss *et al*., "Effects of probe damage on wire bond integrity", *2001 Proceedings. 51st Electronic Components and Technology Conference (Cat. No.01CH37220)*, 2001, pp. 1175-1180, doi: 10.1109/ECTC.2001.927975.

[14] W. Sauter *et al*., "Problems with wirebonding on probe marks and possible solutions", *53rd Electronic Components and Technology Conference, 2003. Proceedings.*, 2003, pp. 1350-1358, doi: 10.1109/ECTC.2003.1216470.

[15] Qing Tan, C. Beddingfield, and A. Mistry, "Reliability evaluation of probe-before-bump technology", *Twenty Fourth IEEE/CPMT Int'l Electronics Manufacturing Tech. Symp. (Cat. No.99CH36330)*, 1999, pp. 320-324, doi: 10.1109/IEMT.1999.804839.

[16] M. J. Varnau, "Impact of wafer probe damage on flip chip yields and reliability", *Nineteenth IEEE/CPMT International Electronics Manufacturing Technology Symposium*, 1996, pp. 293-297, doi: 10.1109/IEMT.1996.559745.

[17] M. Vidal-Dho *et al*., "Probing impact on pad moisture tightness: A challenge for pad size reduction", *2019 IEEE 32nd International Conference on Microelectronic Test Structures (ICMTS)*, 2019, pp. 176-179, doi: 10.1109/ICMTS.2019.8730990.

[18] D. Hall, B. Smith, D. Pechonis, M. Nelson and G. Tranquillo, "Procedure for Controlling Pad Scrub During High-Temperature Wafer Probing", *2022 IEEE 34th Int'l Conf. on Microelectronic Test Structures (ICMTS)*, 2022, pp. 1-3, doi: 10.1109/ICMTS50340.2022.9898166.

[19] J. Frankel and K. Duckworth, "Automated Thermal Drift Correction of Discrete Probes on Motorized Positioners for Device Characterization", *SW Test Workshop*, Jun 2016